The Astrophysical Journal, 703:1338–1345, 2009 October 1 doi:10.1088/0004-637X/703/2/1338

IMAGING ATOMIC AND HIGHLY EXCITED MOLECULAR GAS IN A $z = 6.42$ QUASAR HOST GALAXY: COPIOUS FUEL FOR AN EDDINGTON-LIMITED STARBURST AT THE END OF COSMIC REIONIZATION

Dominik A. Riechers[1,2,7], Fabian Walter[2], Frank Bertoldi[3], Christopher L. Carilli[4], Manuel Aravena[3], Roberto Neri[5], Pierre Cox[5], Axel Weiß[6], and Karl M. Menten[6]

[1] Astronomy Department, California Institute of Technology, MC 249-17, 1200 East California Boulevard, Pasadena, CA 91125, USA; dr@caltech.edu
[2] Max-Planck-Institut für Astronomie, Königstuhl 17, Heidelberg, D-69117, Germany
[3] Argelander Institut für Astronomie, Universität Bonn, Auf dem Hügel 71, Bonn, D-53121, Germany
[4] National Radio Astronomy Observatory, P.O. Box O, Socorro, NM 87801, USA
[5] Institut de Radio Astronomie Millimétrique, 300 Rue de la Piscine, Domaine Universitaire, 38406 Saint Martin d'Héres, France
[6] Max-Planck-Institut für Radioastronomie, Auf dem Hügel 69, Bonn, D-53121, Germany
Received 2008 December 28; accepted 2009 August 10; published 2009 September 9

ABSTRACT

We have imaged CO($J = 7\rightarrow6$) and C I($^3P_2\rightarrow{}^3P_1$) emission in the host galaxy of the $z = 6.42$ quasar SDSS J114816.64+525150.3 (hereafter J1148+5251) through observations with the Plateau de Bure Interferometer. The region showing CO($J = 7\rightarrow6$) emission is spatially resolved, and its size of 5 kpc is in good agreement with earlier CO($J = 3\rightarrow2$) observations. In combination with a revised model of the collisional line excitation in this source, this indicates that the highly excited molecular gas traced by the CO $J = 7\rightarrow6$ line is subthermally excited (showing only 58% ± 8% of the CO $J = 3\rightarrow2$ luminosity), but not more centrally concentrated. We also detect C I($^3P_2\rightarrow{}^3P_1$) emission in the host galaxy of J1148+5251, but the line is too faint to enable a reliable size measurement. From the C I($^3P_2\rightarrow{}^3P_1$) line flux, we derive a total atomic carbon mass of $M_{\rm C\,I} = 1.1\times10^7\ M_\odot$, which corresponds to $\sim5\times10^{-4}$ times the total molecular gas mass. We also searched for $H_2O(J_{K_aK_c} = 2_{12}\rightarrow1_{01})$ emission, and obtained a sensitive line luminosity limit of $L'_{\rm H_2O} < 4.4\times10^9$ K km s^{-1} pc^2, i.e., <15% of the CO($J = 3\rightarrow2$) luminosity. The warm, highly excited molecular gas, atomic gas and dust in this quasar host at the end of cosmic reionization maintain an intense starburst that reaches surface densities as high as predicted by (dust opacity) Eddington limited star formation over kiloparsec scales.

Key words: cosmology: observations – galaxies: active – galaxies: formation – galaxies: high-redshift – galaxies: starburst – radio lines: galaxies

Online-only material: color figures

1. INTRODUCTION

Detailed studies of individual quasars at the highest redshifts are vital to shed light on how today's most massive galaxies are formed and to investigate whether or not the tight correlation between black hole mass and stellar bulge mass seen today was already in place during the earliest stages of galaxy formation. A particularly insightful example is the very high-redshift quasar J1148+5251 ($z = 6.42$), which is observed at the end of cosmic reionization, only ~870 Myr after the big bang.[8] Since its initial discovery in the Sloan Digital Sky Survey (SDSS; Fan et al. 2003), it has been found to be an optical point source even at the resolution achieved by the *Hubble Space Telescope* (*HST*; White et al. 2005), with ultraviolet to infrared colors typical for a type 1 quasar (e.g., Jiang et al. 2006). From its bright and broad Mg II (λλ2796,2803 Å) emission line, a supermassive black hole mass of $3\times10^9\ M_\odot$ has been derived (Willott et al. 2003). It also hosts a $4.2\times10^8\ M_\odot$ reservoir of dust that exhibits a high far-infrared (FIR) continuum luminosity of $L_{\rm FIR} = 2.2\times10^{13}\ L_\odot$ (Bertoldi et al. 2003a; Beelen et al. 2006).

Subsequently, J1148+5251 was detected in molecular gas emission (carbon monoxide, CO; Walter et al. 2003; Bertoldi et al. 2003b), revealing a massive molecular gas reservoir of $2.4\times10^{10}\ M_\odot$ that could fuel star formation and feed the active galactic nucleus (AGN) in this system. High-resolution follow-up observations revealed that this gas is centered on the AGN, but distributed on scales of 5 kpc (Walter et al. 2004). This large molecular reservoir harbors a compact 1.5 kpc size region that emits bright emission from the [C II]($^3P_{3/2}\rightarrow{}^3P_{1/2}$) interstellar medium (ISM) cooling line, which is presumably due to active star formation at an enormous star formation rate (SFR) surface density of $\sim1000\ M_\odot$ yr^{-1} kpc^{-2} (Walter et al. 2009a). The dense, star-forming molecular gas component as traced by hydrogen cyanide (HCN) is comparatively faint, given the source's high SFR and FIR luminosity (Riechers et al. 2007).

In addition, it was found that J1148+5251 is radio-quiet and follows the radio–FIR correlation for star-forming galaxies, providing additional evidence that the FIR dust emission is dominantly heated by young stars rather than the AGN (Carilli et al. 2004; Wang et al. 2008). To further investigate on which scales the star formation takes place, we here aimed at resolving the neutral atomic and the warm, highly excited molecular gas components in the host galaxy of this unique quasar.

2. OBSERVATIONS

We observed the CO($J = 7\rightarrow6$) ($\nu_{\rm rest} = 806.6518$ GHz), C I($^3P_2\rightarrow{}^3P_1$) (809.3435 GHz), and $H_2O(J_{K_aK_c} = 2_{12}\rightarrow1_{01})$ (1669.9048 GHz) emission lines toward J1148+5251 using the IRAM Plateau de Bure Interferometer (PdBI). At $z = 6.419$, these lines are redshifted to 108.7278, 109.0907, and 225.0849 GHz (2.8 and 1.3 mm). First observations were carried out with the PdBI's previous generation receivers in the old 6D configuration in 2003 May, June, and November (May

[7] Hubble Fellow.
[8] We use a concordance, flat ΛCDM cosmology throughout, with $H_0 = 71$ km s^{-1} Mpc^{-1}, $\Omega_{\rm M} = 0.27$, and $\Omega_\Lambda = 0.73$ (Spergel et al. 2007).

observations published by Bertoldi et al. 2003b), and in 2004 April–June and September–November (23 tracks total). Further observations were carried out with the new generation receivers in the new 6A configuration (longest baseline: 760 m) in 2007 February and March (seven tracks total). All tracks were taken under good 3 mm observing conditions. Of the tracks taken with dual frequency setup in 2003/2004, 12 were taken under conditions sufficient for 1 mm observing. The nearby source 1150+497 (distance to J1148+5251: 3.°4) was observed every 22.5 minutes for pointing, secondary amplitude, and phase calibration. For primary flux calibration, several nearby standard calibrators were observed during all runs, leading to a calibration that is accurate within 10%–15% (3 mm) and 15%–20% (1 mm), respectively.

Observations with the previous generation receivers were set up using a total bandwidth of 580 MHz (single polarization, dual frequency; corresponding to ∼1600 km s^{-1} at 2.8 mm and ∼770 km s^{-1} at 1.3 mm). This setup requires two separate tunings at 3 mm to observe the CO($J = 7\rightarrow6$) (14 tracks) and C I($^3P_2\rightarrow{}^3P_1$) (nine tracks) emission lines (1 mm receivers were tuned to the redshifted H_2O $J_{K_aK_c} = 2_{12}\rightarrow1_{01}$ frequency). Observations with the new generation receivers were set up using a total bandwidth of 1 GHz (dual polarization; corresponding to ∼2800 km s^{-1} at 2.8 mm). This setup allows to observe the CO($J = 7\rightarrow6$) and C I($^3P_2\rightarrow{}^3P_1$) lines simultaneously (selecting a tuning frequency of 108.894 GHz centered between both lines). All observations were taken with sufficient bandwidth to cover the underlying continuum simultaneously.

For data reduction and analysis, the IRAM GILDAS package was used. All data were mapped using "natural" weighting unless mentioned otherwise. The CO($J = 7\rightarrow6$) data result in a final rms of 0.33 mJy beam^{-1} per 28 km s^{-1} channel (resolution: 1.″38 × 1.″17). To optimize the spatial resolution, these data were also mapped using "uniform" weighting, leading to a synthesized clean beam size of 0.″86 × 0.″61 (4.8 kpc × 3.4 kpc) and an rms of 0.12 mJy beam^{-1} over 414 km s^{-1} (150 MHz). To maximize the signal-to-noise ratio (S/N), the C I($^3P_2\rightarrow{}^3P_1$) data were tapered to a resolution of 2.″78 × 2.″42, leading to an rms of 0.17 mJy beam^{-1} over 316 km s^{-1} (115 MHz). The 2.8 mm continuum data (combined from all CO $J = 7\rightarrow6$ and C I $^3P_2\rightarrow{}^3P_1$ observations) result in a 1.″20 × 0.″99 beam and an rms of 0.046 mJy beam^{-1} over 563.75 MHz. The H_2O($J_{K_aK_c}$ $= 2_{12}\rightarrow1_{01}$) data result in an rms of 0.76 mJy beam^{-1} over 303 km s^{-1} (227.5 MHz), and the (double sideband) 1.3 mm continuum data result in an rms of 0.34 mJy beam^{-1} over 2 × 563.75 MHz.

3. RESULTS

In Figure 1, the velocity-integrated CO($J = 7\rightarrow6$) emission is shown at a linear resolution of ∼4 kpc (0.″7). From elliptical Gaussian fitting to the 11σ detection of the source in the u–v plane, it is found that the emission is spatially resolved on a scale of 0.″9 ± 0.″16 (5.0 kpc) in the north–south direction, and marginally resolved (0.″54 ± 0.″11; 3.0 kpc) in east–west direction. The peak, extent,[9] and orientation of the emission are in remarkable agreement with the lower-excitation CO($J = 3\rightarrow2$) line emission (color scale in Figure 1; Walter et al. 2004), and the peak is coincident with the position of the optical quasar (cross in Figure 1; White et al. 2005). This demonstrates that the relative astrometry between the CO($J = 7\rightarrow6$) PdBI and CO($J = 3\rightarrow2$) VLA observations is accurate within <0.″1. It also indicates that, even though the CO($J = 7\rightarrow6$) line is only subthermally excited (see discussion below), the emission is apparently *not* more centrally concentrated than the CO($J = 3\rightarrow2$) emission.

In Figure 2, the spectrum of the CO($J = 7\rightarrow6$) emission is shown. The line is detected at a peak flux of $S_\nu = 1.99 \pm 0.23$ mJy and a width of 297 ± 35 km s^{-1}, leading to an integrated line flux of 0.63 ± 0.06 Jy km s^{-1}, and a line luminosity of $L'_{\rm CO(7-6)} = 1.7 \pm 0.2 \times 10^{10}$ K km s^{-1} pc^2

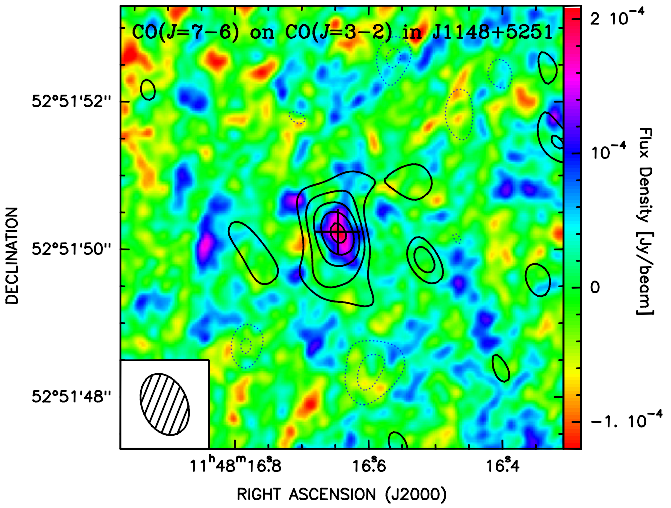

Figure 1. Velocity-integrated PdBI map of the CO($J = 7\rightarrow6$) line emission toward J1148+5251 (contours) over the central 414 km s^{-1}, overlayed on the VLA CO($J = 3\rightarrow2$) map (Walter et al. 2004; color scale). At a resolution of 0.″86 ×0.″61, the emission is resolved. The cross indicates the position of the optical quasar (White et al. 2005). Contours are shown at (−3, −2, 2, 3, 4, 5, 6)×σ (1σ = 0.125 mJy beam^{-1}).

(A color version of this figure is available in the online journal.)

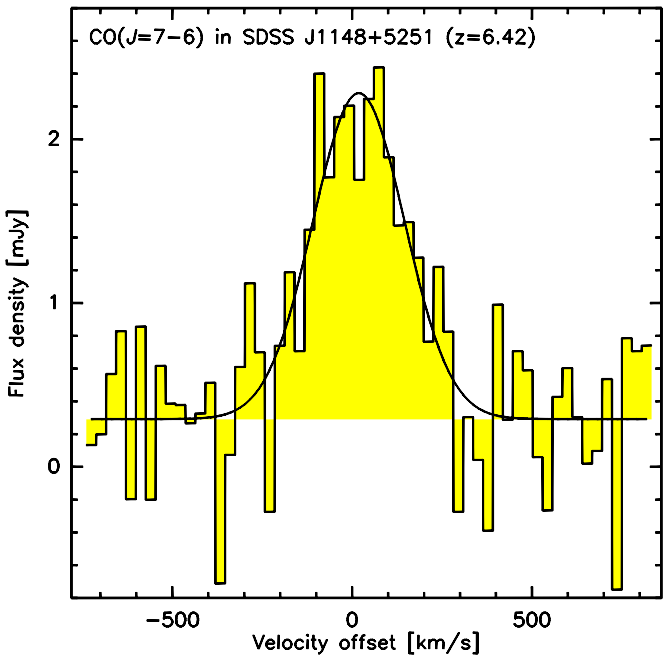

Figure 2. PdBI spectrum of the CO($J = 7\rightarrow6$) and underlying 2.8 mm continuum emission toward J1148+5251 at a resolution of 28 km s^{-1} (10 MHz). The velocity scale is relative to the redshifted CO($J = 7\rightarrow6$) frequency at z = 6.419. The rms per velocity bin is 0.33 mJy. The solid line shows a Gaussian fit to the data.

(A color version of this figure is available in the online journal.)

[9] Accounting for beam convolution.

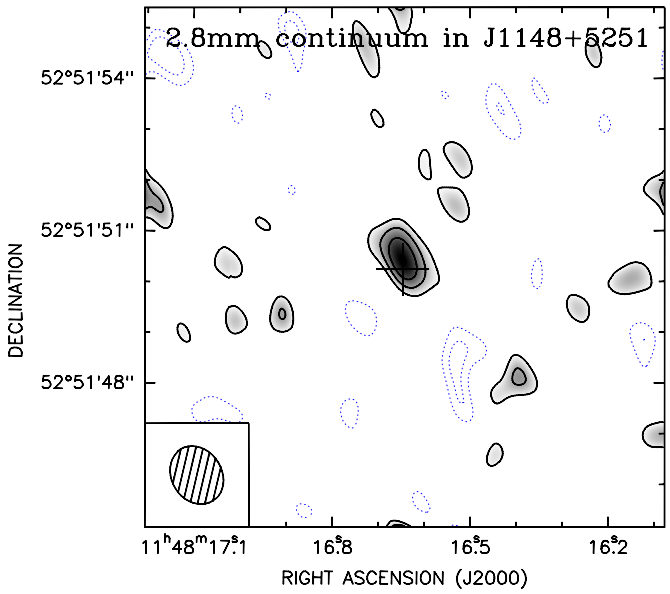

Figure 3. Map of the 2.8 mm continuum emission toward J1148+5251. At 1.″20 × 0.″99 resolution, the emission appears unresolved. Contours are shown at (−3, −2, 2, 3, 4, 5)×σ (1σ = 0.046 mJy beam^{-1}). The cross indicates the same position as in Figure 1.

(A color version of this figure is available in the online journal.)

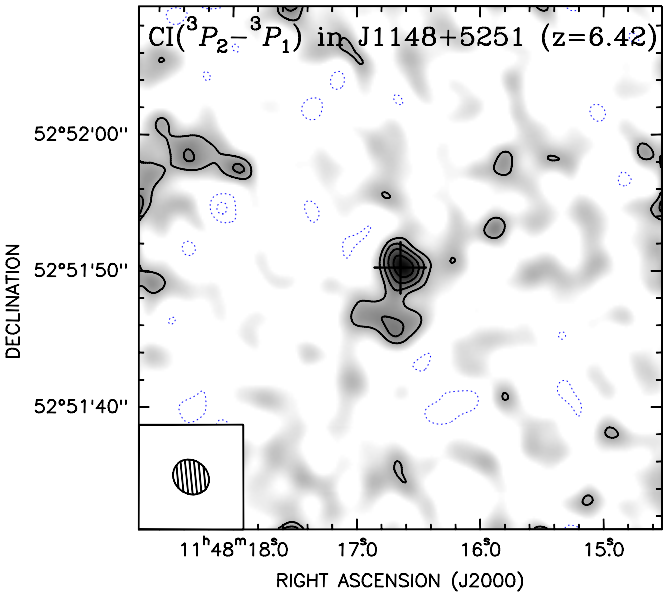

Figure 4. Velocity-integrated map of the C I($^3P_2\rightarrow{}^3P_1$) line emission over 316 km s^{-1} toward J1148+5251. At 2.″78 × 2.″42 resolution, the emission appears unresolved. Contours are shown at (−3, −2, 2, 3, 4, 5)×σ (1σ = 0.167 mJy beam^{-1}). The cross indicates the same position as in Figure 1.

(A color version of this figure is available in the online journal.)

Table 1
Line Fluxes and Luminosities in SDSS J1148+5251

	$S_\nu dv$ (Jy km s^{-1})	L' (10^9 K km s^{-1} pc^2)	References
CO($J=1\rightarrow0$)	<0.11	<143	1
CO($J=3\rightarrow2$)	0.20 ± 0.02	29.9 ± 2.7	2
CO($J=6\rightarrow5$)	0.67 ± 0.08	25.0 ± 3.0	1
CO($J=7\rightarrow6$)	0.63 ± 0.06	17.2 ± 1.8	1,3
HCN($J=2\rightarrow1$)	<0.006	<3.3	4
HCO$^+$($J=2\rightarrow1$)	<0.018	<10	5
$H_2O(J_{K_aK_c}=2_{12}\rightarrow1_{01})$	<0.69	<4.4	3
C I($^3P_2\rightarrow{}^3P_1$)	0.22 ± 0.05	6.0 ± 1.3	3
[C II]($^3P_{3/2}\rightarrow{}^3P_{1/2}$)	3.9 ± 0.3	19.0 ± 1.6	6,7
[N II]($^3P_1\rightarrow{}^3P_0$)	<0.47	<4.0	8

Notes. CO($J=3\rightarrow2$) corrected by 10% to account for flux in the outer linewings not covered by the observations. Line fluxes are continuum-corrected where applicable.

References. (1) Bertoldi et al. 2003b; (2) Walter et al. 2003; (3) this work; (4) Riechers et al. 2007; (5) Carilli et al. 2005; (6) Maiolino et al. 2005; (7) Walter et al. 2009a; (8) Walter et al. 2009b.

(see Table 1). The sensitivity of the observations is sufficient to detect, for the first time, the underlying 2.8 mm continuum emission (0.28 ± 0.07 mJy). Figure 3 shows a map of the 2.8 mm continuum emission integrated over all line-free channels of the *combined* CO and C I observations at ∼6 kpc (1.″1) linear resolution. The continuum emission is detected at a flux level consistent with the simultaneous line/continuum fit to the CO(J = 7→6) spectrum within the errors.

In Figure 4, a velocity-integrated map of the C I($^3P_2\rightarrow{}^3P_1$) emission over 316 km s^{-1} (i.e., approximately the CO line FWHM) is shown at a linear resolution of ∼15 kpc (2.″6). Emission is detected at 0.98 ± 0.17 mJy peak flux, corresponding to a line peak flux of 0.7 mJy when accounting for the underlying continuum. This corresponds to an integrated C I($^3P_2\rightarrow{}^3P_1$) line flux of 0.22 ± 0.05 Jy km s^{-1}, and a line luminosity of $L'_{\rm C\,I(2-1)}$ = 6.0 ± 1.3 × 10^9 K km s^{-1} pc^2. At higher spatial resolution, the line is still marginally detected, but the peak flux decreases. This may indicate that the C I($^3P_2\rightarrow{}^3P_1$) emission is resolved on similar scales as the CO emission, and thus emerges from the same (molecular) gas phase on global (galactic) scales. However, this conclusion remains tentative at the present S/N.

No evidence for $H_2O(J_{K_aK_c}=2_{12}\rightarrow1_{01})$ emission is found in the 1.3 mm data. Assuming that the line has the same width as CO(J = 7→6), we derive a 3σ upper limit of <0.69 Jy km s^{-1} for the integrated line flux, and a line luminosity limit of $L'_{\rm H_2O}$ <4.4 × 10^9 K km s^{-1} pc^2 (i.e., $L'_{\rm H_2O}/L'_{\rm CO(3-2)}$ < 0.15). We clearly detect the underlying 225 GHz continuum emission at 3.9 ± 0.8 mJy.

4. DISCUSSION

4.1. Properties of the Molecular and Atomic ISM in J1148+5251

4.1.1. Resolved CO(J = 7→6) Emission

We successfully resolved emission from the high-J CO(J = 7→6) line toward the z = 6.42 quasar J1148+5251. The structure and size of the gas reservoir are consistent with what was derived from previous CO(J = 3→2) line mapping (Walter et al. 2004). The line width derived from our high S/N CO(J = 7→6) spectrum is consistent with that of previous observations of the CO(J = 6→5) and CO(J = 7→6) lines (Bertoldi et al. 2003b). Although the molecular gas emission appears to be more extended than that from the neutral ISM as traced by the 158 μm [C II]($^3P_{3/2}\rightarrow{}^3P_{1/2}$) line, the linewidths and centroids are consistent to high precision (Maiolino et al. 2005; Walter et al. 2009a).

4.1.2. Atomic Carbon

We also detected the upper fine structure line of neutral carbon, C I($^3P_2\rightarrow{}^3P_1$), toward J1148+5251. This represents the highest z detection of atomic carbon (or, indeed, any neutral atomic medium) to date, and the first C I detection in an unlensed high-redshift galaxy. As the lower fine structure line (which

is redshifted to 66.3 GHz) cannot be observed with current facilities, it is not possible to derive an excitation temperature for C I. However, for $T_{ex} > 20$ K, the derived C I mass only weakly depends on T_{ex} (Weiß et al. 2005a). Assuming an excitation temperature of $T_{ex} = 36$ K (the average of the Cloverleaf and IRAS F10214+4724, the only high-z galaxies for which both transitions have been detected; Barvainis et al. 1997; Weiß et al. 2003, 2005a; Ao et al. 2008), we derive a C I mass of $M_{C\,I} = 1.1 \times 10^7\ M_\odot$. From the CO luminosity, a total molecular gas mass of $M_{H_2} = 2.4 \times 10^{10}\ M_\odot$ can be derived (Walter et al. 2003).[10] We thus find a C I/H_2 mass fraction of 5×10^{-4}. Assuming a [C I]/[H_2] abundance ratio of 5×10^{-5} (Weiß et al. 2003, 2005a), the C I mass translates to a total molecular gas mass of $M_{H_2} = 3.7 \times 10^{10}\ M_\odot$. This is somewhat higher than the value derived from the CO luminosity, and may indicate either a higher atomic carbon abundance, or that the CO luminosity to H_2 mass conversion factor is higher than that assumed above (possibly due to different *molecular* abundances relative to nearby ultra-luminous infrared galaxies (ULIRGs)).

By comparing the line luminosities (in units of $L_\odot$), one finds that the C I($^3P_2 \rightarrow {}^3P_1$) line provides only ~2% of the cooling capacity of the [C II]($^3P_{3/2} \rightarrow {}^3P_{1/2}$) line (Maiolino et al. 2005; Walter et al. 2009a); the latter thus clearly remains the strongest detected coolant of the neutral atomic ISM. This also implies $L_{C\,I}/L_{FIR} \simeq 5 \times 10^{-6}$. This ratio is comparable to those found in nearby star-forming and starbursting galaxies, where it is considered to be a measure for the strength of the non-ionizing stellar UV radiation field (e.g., Gérin & Philips 2000; Bayet et al. 2006). This supports the assumption that the bulk of the dust and gas heating in this system is powered by star formation. Together with the $L_{C\,II}/L_{FIR}$ ratio of $\sim 2 \times 10^{-4}$ (Walter et al. 2009a), the above ratios imply that the UV radiation field in J1148+5251 is relatively strong, and that the gas density is high (as predicted by photodissociation region (PDR) models), consistent with nearby ULIRGs like Arp 220 (Gérin & Philips 2000, their Figure 8).

4.1.3. Limits on Water Emission

We have also searched for $H_2O(J_{K_aK_c} = 2_{12} \rightarrow 1_{01})$ emission toward J1148+5251, but only obtained a sensitive upper limit. Radiative transfer calculations show that, assuming the known gas and dust properties of J1148+5251, $H_2O(J_{K_aK_c} = 2_{12} \rightarrow 1_{01})$ emission is expected to be optically thick over a substantial range of the permitted parameter space. Thus, the line luminosity limit can be directly translated to a surface filling factor limit (relative to CO $J = 3 \rightarrow 2$) of <15% (assuming both lines are in thermal equilibrium).

Sensitive searches for water emission from dense molecular gas were performed for two other $z > 3$ galaxies (Riechers et al. 2006a; Wagg et al. 2006), reaching comparable depths. A search for $H_2O(J_{K_aK_c} = 3_{13} \rightarrow 2_{20})$ emission ($\nu_{rest} = 183.310$ GHz) toward the $z = 3.20$ quasar MG 0751+2716 provided a surface filling factor limit of <6% relative to CO($J = 4 \rightarrow 3$) (assuming the same conditions; Riechers et al. 2006a). A search for $H_2O(J_{K_aK_c} = 1_{10} \rightarrow 1_{01})$ emission ($\nu_{rest} = 556.936$ GHz) toward the $z = 3.91$ quasar APM 08279+5255 provided a surface filling factor limit of <12% relative to CO($J = 4 \rightarrow 3$) (Wagg et al. 2006; Weiß et al. 2007a; Riechers et al. 2009).

Note that the $H_2O(J_{K_aK_c} = 3_{13} \rightarrow 2_{20})$ transition was detected toward the nearby ULIRG Arp 220, at about one third of its HCN($J = 1 \rightarrow 0$) line luminosity (Cernicharo et al. 2006). This suggests a small surface filling factor even within dense molecular cloud cores as traced by HCN. This is, again, assuming optically thick emission in thermal equilibrium from both lines. Note that the H_2O line emission in Arp 220 (and the high-z sources) is likely maser-enhanced, which would even predict substantially smaller surface filling factors (Cernicharo et al. 2006; Riechers et al. 2006a). Although different H_2O and HCN transitions were observed toward J1148+5251, the observed $H_2O(J_{K_aK_c} = 2_{12} \rightarrow 1_{01})$ luminosity limit would be consistent with a H_2O/HCN line luminosity ratio similar to Arp 220.

4.2. Continuum Emission

The new detections of the observed-frame 225 GHz (rest-frame: 1.67 THz) and 109 GHz (807 GHz) continuum emission are consistent with the overall dust spectral energy distribution (SED) of J1148+5251 (Beelen et al. 2006). In particular, the detection of 2.8 mm continuum emission allows us to better constrain both the CO($J = 7 \rightarrow 6$) and CO($J = 6 \rightarrow 5$) line fluxes. From the shape of the SED, we derive an estimated continuum flux of 0.19 mJy at the wavelength of the CO($J = 6 \rightarrow 5$) emission, by which we reduce the CO($J = 6 \rightarrow 5$) flux relative to the original estimate (Bertoldi et al. 2003b) in the following.

5. MODELING AND CONCLUSIONS

5.1. CO Line Excitation

Given the high S/N of the CO($J = 7 \rightarrow 6$) observations and the fact that we successfully detected the (observed-frame) 2.8 mm continuum emission (which also provided an updated CO($J = 6 \rightarrow 5$) line flux), we have calculated new large velocity gradient (LVG) models of the line excitation in this system (see Bertoldi et al. 2003b for the original study). In this LVG model study, the kinetic gas temperature and density are treated as free parameters. For all calculations, the H_2 ortho-to-para ratio was fixed to 3:1,[11] the cosmic microwave background temperature was fixed to 20.25 K (at $z = 6.42$), and the Flower (2001) CO collision rates were used. We adopted a CO abundance per velocity gradient[12] of $[CO]/(dv/dr) = 1 \times 10^{-5}$ pc (km s^{-1})$^{-1}$ (e.g., Weiß et al. 2005c, 2007a; Riechers et al. 2006b), and a CO disk radius of 2.5 kpc as found from the spatially resolved CO($J = 3 \rightarrow 2$) and CO($J = 7 \rightarrow 6$) observations. The best solution was obtained for a spherical, single-component model with a CO disk filling factor of 0.16, $T_{kin} = 50$ K, and $\rho_{gas}(H_2) = 10^{4.2}$ cm^{-3} (Figure 5). These values are comparable to those found for other high-z quasars (e.g., Riechers et al. 2006b; Weiß et al. 2007b). This model predicts that the CO($J = 3 \rightarrow 2$) line emission is thermalized. Also, the model-predicted gas

[10] CO in high-z quasar hosts is more widespread than in nearby ULIRGs, but shows similar physical properties. We thus adopt a low ULIRG CO luminosity to H_2 mass conversion factor of $\alpha = 0.8\ M_\odot$ (K km s^{-1} pc^2)$^{-1}$ (Downes & Solomon 1998) rather than $\alpha = 4$–$5\ M_\odot$ (K km s^{-1} pc^2)$^{-1}$ as in nearby spirals (e.g., Scoville & Sanders 1987; Solomon & Barrett 1991). Such low α are also found for $z \sim 2.5$ submillimeter galaxies (Tacconi et al. 2008).

[11] This is due to the relative statistical weights of the symmetrical (ortho) and antisymmetrical (para) eigenstates of the wavefunction: there are three symmetrical combinations of the spins of both H nuclei, but there is only one antisymmetrical combination.

[12] Only the ratio of [CO] and dv/dr enters the LVG calculations. Thus, our solutions can account for the factor of a few variations in [CO] found between nearby star-forming galaxies by adjusting the "internal" parameter dv/dr accordingly. Here, $[CO]/(dv/dr)$ is fixed to that of the nearby starburst M82 (Weiß et al. 2005c).

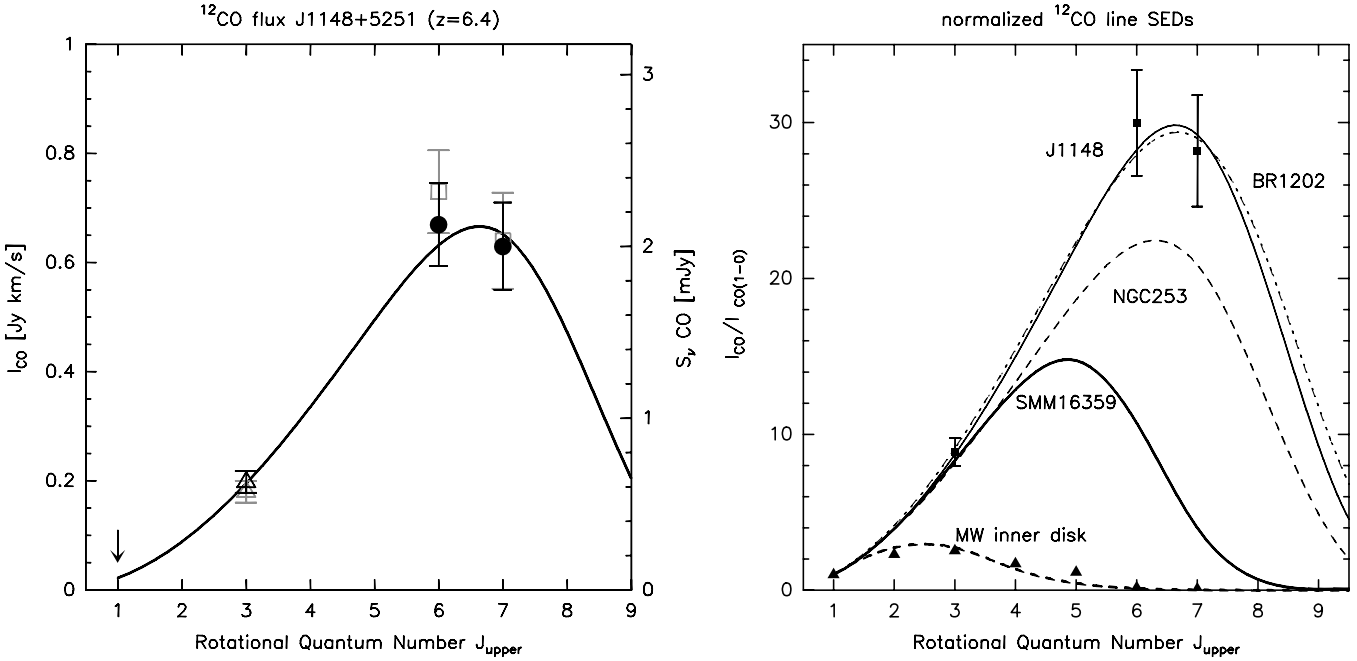

Figure 5. Left: CO excitation ladder (points) and LVG model (line) for J1148+5251. The upper limit for CO($J = 1\rightarrow0$) and the (continuum corrected) data point for CO($J = 6\rightarrow5$) are taken from Bertoldi et al. (2003b). The CO($J = 3\rightarrow2$) data point (corrected for missing flux in the line wings) is taken from Walter et al. (2003). The grey points indicate the original, uncorrected fluxes from Bertoldi et al. (2003b). The model predicts kinetic temperatures and gas densities of $T_{kin} = 50$ K and $\rho_{gas}(H_2) = 10^{4.2}$ cm^{-3}. Right: Comparison of the normalized excitation ladders for different sources: the inner disk of the Milky Way (triangles and thick dashed line; Fixsen et al. 1999), the $z = 2.5$ submillimeter galaxy SMM J16359+6612 (thick solid line; Weiß et al. 2005b), the nearby starburst galaxy NGC 253 (dashed line; Güsten et al. 2006), the $z = 4.7$ quasar BR 1202-0725 (dash-dotted line; Riechers et al. 2006b), and J1148+5251 (squares and solid line).

temperature is consistent with that of the dust (55 ± 5 K; Beelen et al. 2006).

5.2. Star Formation Rate and its Surface Density

The dust reservoir in J1148+5251 exhibits a FIR continuum luminosity of $L_{FIR} = 2.2 \times 10^{13}\ L_\odot$ (Bertoldi et al. 2003a; Beelen et al. 2006), about half of which emerges from a compact, 0.75 kpc radius region (Walter et al. 2009a). Its molecular gas, dense gas, radio continuum, and dust properties are consistent with L_{FIR} being dominantly powered by star formation (e.g., Beelen et al. 2006; Riechers et al. 2007; Walter et al. 2009a). Assuming that the AGN contribution to L_{FIR} is small, we thus derive[13] an integrated SFR of 3300 $M_\odot$ yr^{-1}, about half of which takes place within a 0.75 kpc radius region. This high SFR is consistent with the high luminosity of the [C II]($^3P_{3/2}\rightarrow{}^3P_{1/2}$) ISM cooling line (Maiolino et al. 2005), which emerges from a region of 0.75 kpc radius within the molecular gas reservoir (Walter et al. 2009a). An intense, kpc-scale starburst is also needed to explain the fact that the molecular gas is warm and highly excited over a large, 5 kpc size region (as shown by the new, spatially resolved CO $J = 7\rightarrow6$ data), which requires a heating source of similar size (given that radiation from a compact heating source such as the AGN likely cannot penetrate the dense molecular reservoir out to such large scales).

Thus, the (peak) size and brightness of the resolved [C II]($^3P_{3/2}\rightarrow{}^3P_{1/2}$) line and FIR continuum emission are consistent with a nuclear "hyper"-starburst as the main heating source for the gas and dust, i.e., a starburst that exhibits a flux of $F_{FIR} = 10^{13}\ L_\odot$ kpc^{-2}, produced by an enormous SFR surface density of $\Sigma_{SFR} = 1000\ M_\odot$ yr^{-1} kpc^{-2} (Walter et al. 2009a). Such high F_{FIR} and Σ_{SFR} are typically observed in the most extreme star-forming environments in the local universe. As a reference, the Galactic star forming cloud Orion exhibits a FIR luminosity of $1.2 \times 10^5\ L_\odot$ within its central arcmin^2 (0.013 pc^2; Werner et al. 1976). This corresponds to a F_{FIR} of $\sim10^{13}\ L_\odot$ kpc^{-2}. Nearby ULIRGs exhibit a FIR luminosity of typically $3 \times 10^{11}\ L_\odot$ within their most active $\sim$100 pc size regions (Downes & Solomon 1998). This, again, corresponds to a F_{FIR} of $\sim10^{13}\ L_\odot$ kpc^{-2}. F_{FIR} (or Σ_{SFR}) as extreme as in J1148+5251 thus are observed in the Galaxy and the local universe, albeit in areas that are by 2–8 orders of magnitude smaller. Over surface areas comparable to J1148+5251, extreme starbursts at $z > 2$ (submillimeter galaxies, SMGs) have typical Σ_{SFR} of $\sim80\ M_\odot$ yr^{-1} kpc^{-2} (Tacconi et al. 2006), which are by about an order of magnitude smaller.

Intriguingly, recent high-resolution molecular gas and radio continuum observations of the $z = 4.4$ merging quasar host of BRI 1335-0417 indicate Σ_{SFR} comparable to those in J1148+5251 (assuming that the FIR-emitting dust is not more extended than the molecular gas; Riechers et al. 2008b; Momjian et al. 2007).

5.3. Radiation–Pressure Supported Starburst Disks

An SFR surface density of $\Sigma_{SFR} = 1000\ M_\odot$ yr^{-1} kpc^{-2} is consistent with theories of "maximum starbursts" (Elmegreen 1999). At such high surface densities, feedback from star formation is likely to occur, which may (self-)regulate the starburst. If the maximum intensity of a radiation pressure-supported, galaxy scale starburst is determined by the Eddington limit for dust, a number of characteristic limits arise in these "maximum starburst" theories (Thompson et al. 2005). Assuming a Salpeter-like initial mass function (IMF), a constant gas-to-dust ratio with radius, and that the disk is self-regulated (i.e., Toomre-Q $\sim$1), such an Eddington-limited starburst has

[13] Assuming SFR=$1.5 \times 10^{-10}\ L_{FIR}(M_\odot\ \mathrm{yr}^{-1}/L_\odot)$ (Kennicutt 1998).

$\Sigma_{\rm SFR} \sim 1000\,M_\odot$ yr^{-1} kpc^{-2}, $F_{\rm FIR} \sim 10^{13}\,L_\odot$ kpc^{-2}, and an effective temperature of 88 K (using Equations (34)–(36) of Thompson et al. 2005). As shown above, J1148+5251 has $\Sigma_{\rm SFR}$ and $F_{\rm FIR}$ close to these theoretical limits over a 0.75 kpc radius region.

For a flat disk as assumed here, $F_{\rm FIR} = L_{\rm FIR}/(\pi\, r^2) = \sigma_{\rm SB}\, T_{\rm eff}^4$, where r is the disk radius, and $\sigma_{\rm SB}$ is the Stefan–Boltzmann constant.[14] About half of $L_{\rm FIR}$ comes from a 0.75 kpc radius region in J1148+5251. This corresponds to $T_{\rm eff}^{\rm peak} = 82$ K, which is also consistent with the limit. Note that, integrated over the whole 5 kpc region traced by CO (and full $L_{\rm FIR}$), this simplified calculation predicts $T_{\rm eff} = 53$ K, which is in good agreement with the kinetic temperature of the molecular gas as derived above, and the dust temperature obtained from fitting the SED of the source.

The vertical optical depth of a disk is given by $\tau_V = \Sigma_{\rm gas}\,\kappa/2$, where $\Sigma_{\rm gas}$ is the gas surface density, and $\kappa \simeq \kappa_0\, T_{\rm eff}^2$ (valid for $T_{\rm eff} \lesssim 200$ K; $\kappa_0 \simeq 2.4\times10^{-4}$ cm^2 g^{-1} K^{-2}; see Thompson et al. 2005) is the Rosseland mean opacity for dust. The assumption of a constant gas-to-dust ratio with radius implies that about half of the gas mass is found within a 0.75 kpc radius region in J1148+5251. Together with the $T_{\rm eff}^{\rm peak}$ derived above, this implies $\tau_V = 1.03$ (i.e., moderately optically thick), consistent with the assumptions of the Eddington-limited starburst model.

From the dynamical [C II]($^3P_{3/2}\rightarrow{}^3P_{1/2}$) line map of J1148+5251, we can derive a dynamical mass of $M_{\rm dyn} \sim 1.5 \times 10^{10}\,M_\odot$ within a 0.75 kpc radius region. Assuming that $M_{\rm dyn}$ traces the total mass within that region, this corresponds to a gas mass fraction of $f_{\rm gas} = 0.72$. Using Equation (37) of Thompson et al. (2005), this suggests that the disk is optically thick out to a radius of ~400 pc.[15] This value is by almost a factor of 2 smaller than 750 pc. This may indicate that the potential is not isothermal, as assumed in the model. It may also indicate that the three-dimensional distribution of the gas and dust is more complicated than assumed here. However, the model reproduces a number of the observed properties of J1148+5251 fairly well. Our observations thus are, indeed, consistent with a kiloparsec-scale "maximum starburst," radiating close to its characteristic Eddington limit. This hyper-starburst is harbored by a large, 5 kpc size, overall warm and highly excited molecular gas reservoir that hosts $2.4 \times 10^{10}\,M_\odot$ of molecular hydrogen and $1.1 \times 10^7\,M_\odot$ of atomic carbon.

5.4. Dense Molecular Gas and Gas Surface Density

There are additional lines of evidence that suggest that $\Sigma_{\rm SFR}$ as high as $1000\,M_\odot$ yr^{-1} kpc^{-2} on kpc scales (as observed in J1148+5251) are not unreasonable. Recent investigations of the (in the nearby universe linear) HCN–FIR luminosity correlation at high z (including J1148+5251) show tentative evidence for an excess in $L_{\rm FIR}$ relative to the observed $L'_{\rm HCN}$ toward the highest $L_{\rm FIR}$ systems (both with and without AGN; Carilli et al. 2005; Gao et al. 2007; Riechers et al. 2007). Such an excess can be explained by higher median gas densities (comparable to the critical density of HCN $J = 1\rightarrow0$) in the most FIR-luminous galaxies (Krumholz & Thompson 2007; Narayanan et al. 2008a). Even when assuming a constant efficiency of turning a unit mass of molecular gas into stars among all galaxies, this would imply a higher SFR per unit area for the most FIR-luminous systems.

[14] Assuming a blackbody, which the dust SED only approximates.

[15] As $M_{\rm dyn} \propto \sigma^2_{\rm FWHM}$ was used to determine the gas fraction, this value is independent of the assumed disk inclination.

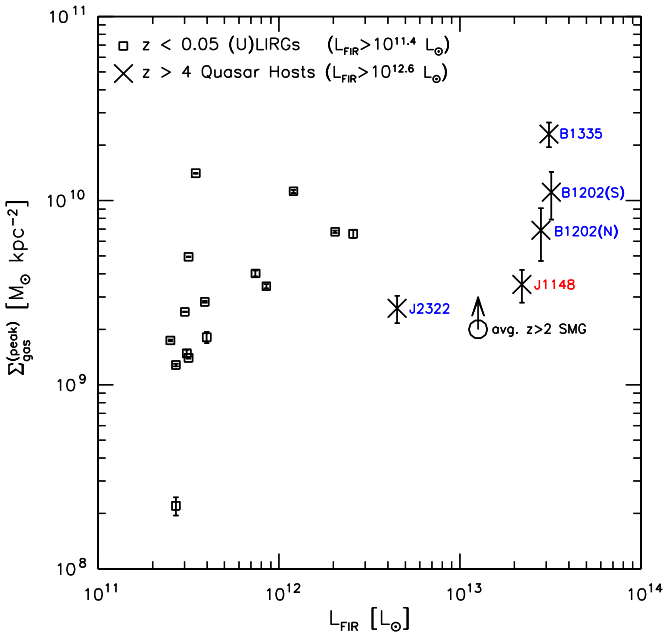

Figure 6. Molecular gas peak surface density ($\Sigma_{\rm gas}^{\rm (peak)}$) as a function of FIR luminosity ($L_{\rm FIR}$) for nearby luminous and ultra-luminous infrared galaxies (squares; Wilson et al. 2008) and $z > 4$ quasar host galaxies (crosses), including PSS J2322+1944 ($z = 4.12$), BRI 1335-0417 ($z = 4.41$), BR 1202-0725 north and south ($z = 4.69$), and J1148+5251 ($z = 6.42$; this work; Carilli et al. 2002; Riechers et al. 2008a, 2008b). Data for J2322+1944 are corrected for gravitational lensing. For comparison, the surface-averaged $\Sigma_{\rm gas}^{R_{1/2}}$ at half intensity radius for $z > 2$ SMGs is shown (circle; sample average of Tacconi et al. 2006).

(A color version of this figure is available in the online journal.)

The (molecular) gas surface density in J1148+5251 consistently reaches high peak values of up to $\Sigma_{\rm gas}^{\rm (peak)} = 3.5 \times 10^9\,M_\odot$ kpc^{-2}. In Figure 6, the $\Sigma_{\rm gas}^{\rm (peak)}$ of J1148+5251, other $z > 4$ quasar host galaxies (Carilli et al. 2002; Riechers et al. 2008a, 2008b), and a sample of nearby LIRGs and ULIRGs (Wilson et al. 2008) is shown as a function of $L_{\rm FIR}$. For comparison, a lower limit for $z > 2$ SMGs is shown (Tacconi et al. 2006). Wilson et al. (2008) suggested that there may be a trend of increasing $\Sigma_{\rm gas}^{\rm (peak)}$ with $L_{\rm FIR}$. This would be consistent with a higher density of gas clouds toward more intensely star-forming galaxies. However, their sample of nearby galaxies spans only about an order of magnitude in $L_{\rm FIR}$. Including the more FIR-luminous high-z systems, this trend gets substantially weaker. In fact, the high-z systems appear to occupy a similar range in $\Sigma_{\rm gas}^{\rm (peak)}$ as the nearby ULIRGs, and the relation appears to saturate close to the typical gas surface densities of giant molecular cloud (GMC) cores. This would imply that, in the most FIR-luminous systems, the entire kiloparsec-scale regions with the highest $\Sigma_{\rm gas}^{\rm (peak)}$ have gas surface densities close to those in GMC cores. One limitation of this conclusion is that the nearby galaxies were studied at a factor 1.8 higher linear (physical) resolution than the $z > 4$ systems. This, however, is not sufficient to explain the weakening of the trend. In particular, the $z = 4.4$ quasar BRI 1335-0417 with the highest $\Sigma_{\rm gas}^{\rm (peak)}$ (Riechers et al. 2008b) was studied at only 20% lower resolution than the nearby sample average. Even assuming conservatively that $\Sigma_{\rm gas}^{\rm (peak)}$ is by ~50% higher in this source (according to the difference in beam area), it is still consistent with that in the nuclei of the nearby ULIRG Arp 220 (Downes & Solomon 1998). This would be consistent

with a picture in which the molecular ISM in ULIRGs and even more FIR-luminous systems is dominantly in a rather dense, relatively continuous phase (rather than in individual, moderately dense molecular clouds), exhibiting optically thick emission. While the measured (peak) gas surface densities are comparable, the gas is spread out over larger areas in the high-z quasar host galaxies relative to the (dense) nuclei of nearby ULIRGs, consistent with the higher total gas masses and SFRs, and higher median gas densities (integrated over the whole galaxies). Overall, this may suggest that a tighter correlation would be found if $\Sigma_{\rm gas}^{\rm (peak)}$ is compared to $\Sigma_{\rm SFR}$ instead of the integrated $L_{\rm FIR}$ (as a proxy of SFR).

5.5. Evolution of the Gaseous and Stellar Components

Assuming that the massive amounts of molecular material available on 5 kpc scales in J1148+5251 are converted into stars at an efficiency of 5%–10% as in GMC cores (e.g., Myers et al. 1986; Scoville et al. 1987), the SFR corresponds to a gas depletion timescale of only (0.7–1.4) $\times$ 10^8 yr. This is about one-third of the value found for BRI 1335-0417 (Riechers et al. 2008b), suggesting a rapid buildup of the stellar component in both galaxies. Still, this gas depletion timescale is a few times larger than the dynamical and free-fall times of both the 0.75 kpc radius region traced by [C II], and the full 5 kpc size molecular reservoir. In this regard, the ongoing star formation may still be considered slow.

The [C II]($^3P_{3/2}\rightarrow{}^3P_{1/2}$) dynamical mass estimate suggests that J1148+5251 hosts a total mass of $\sim$1.5 $\times$ 10^{10} $M_\odot$ within a $\sim$0.75 kpc radius region. A present day, massive elliptical galaxy with a black hole mass comparable to J1148+5251 and a velocity dispersion of 300 km s^{-1} hosts a total mass of $\sim$5–8 $\times$ 10^{10} $M_\odot$ within a central region of the same size (and a total stellar mass of $\sim$2 $\times$ 10^{12} $M_\odot$ distributed over its entire spheroid; e.g., Häring & Rix 2004). Even assuming that the whole amount of molecular material in J1148+5251 were to eventually contribute to the assembly of the stellar spheroid within this small central region leaves a factor of a few difference between the central mass budgets of the $z = 6.42$ quasar and a $z = 0$ massive elliptical galaxy. This suggests that J1148+5251 has to accrete additional material by $z = 0$ (e.g., through subsequent mergers) to grow a spheroid mass comparable to its (likely) present-day counterparts.

On the other hand, the widths of the CO($J = 7\rightarrow6$) and [C II]($^3P_{3/2}\rightarrow{}^3P_{1/2}$) lines are the same within the uncertainties, while the sizes of the CO and [C II]-emitting regions appear to be different by a factor of $\sim$3. Thus, [C II] traces a smaller dynamical mass than CO, corresponding to a shallower potential well. This difference may indicate that the gas in J1148+5251 has not yet fully coalesced, possibly due to an ongoing merger. This would be consistent with the high star formation efficiency found in the central region of this galaxy (Walter et al. 2009a), and the comparatively high fraction of dense gas (Riechers et al. 2007).

We conclude that the highly excited, several kpc scale size gas reservoirs in dust- and gas-rich high-z quasar host galaxies are dominantly heated by the large-scale starbursts that they maintain, consistent with cosmological simulations of merger-driven $z \sim 6$ quasar formation (Li et al. 2008; Narayanan et al. 2008b). These starbursts reach surface densities as predicted by Eddington-limited star formation over kpc scales, accompanied (and probably supported) by ongoing major, "wet" merger activity in some cases.

We thank Todd Thompson, Arjen van der Wel, and Hans-Walter Rix for helpful discussions, the anonymous referee for helpful comments, and Christian Henkel for his LVG code. This research is based on observations carried out with the IRAM PdBI. IRAM is supported by INSU/CNRS (France), MPG (Germany), and IGN (Spain). D.R. acknowledges support from from NASA through Hubble Fellowship grant HST-HF-01212.01-A awarded by the Space Telescope Science Institute, which is operated by the Association of Universities for Research in Astronomy, Inc., for NASA, under contract NAS 5-26555. C.C. acknowledges support from the Max-Planck-Gesellschaft and the Alexander von Humboldt-Stiftung through the Max-Planck-Forschungspreis 2005. D.R. and F.W. appreciate the hospitality at the Aspen Center for Physics, where part of this manuscript was written.

REFERENCES

Ao, Y., et al. 2008, A&A, 491, 747
Barvainis, R., Maloney, P., Antonucci, R., & Alloin, D. 1997, ApJ, 484, 695
Bayet, E., Gerin, M., Phillips, T. G., & Contursi, A. 2006, A&A, 460, 467
Beelen, A., et al. 2006, ApJ, 642, 694
Bertoldi, F., et al. 2003a, A&A, 406, L55
Bertoldi, F., et al. 2003b, A&A, 409, L47
Carilli, C. L., et al. 2002, AJ, 123, 1838
Carilli, C. L., et al. 2004, AJ, 128, 997
Carilli, C. L., et al. 2005, ApJ, 618, 586
Cernicharo, J., Pardo, J. R., & Weiss, A. 2006, ApJ, 646, L49
Downes, D., & Solomon, P. M. 1998, ApJ, 507, 615
Elmegreen, B. G. 1999, ApJ, 517, 103
Fan, X., et al. 2003, AJ, 125, 1649
Fixsen, D. J., et al. 1999, ApJ, 526, 207
Flower, D. R. 2001, J. Phys. B: At. Mol. Opt. Phys., 34, 2731
Gao, Y., Carilli, C. L., Solomon, P. M., & Vanden Bout, P. A. 2007, ApJ, 660, L93
Gérin, M., & Philips, T. G. 2000, ApJ, 537, 644
Güsten, R., Philipp, S. D., Weiß, A., & Klein, B. 2006, A&A, 454, L115
Häring, N., & Rix, H.-W. 2004, ApJ, 604, L89
Jiang, L., et al. 2006, AJ, 132, 2127
Kennicutt, R. C. 1998, ApJ, 498, 541
Krumholz, M. R., & Thompson, T. A. 2007, ApJ, 669, 289
Li, Y., et al. 2008, ApJ, 678, 41
Maiolino, R., et al. 2005, A&A, 440, L51
Momjian, E., Carilli, C. L., Riechers, D. A., & Walter, F. 2007, AJ, 134, 694
Myers, P. C., et al. 1986, ApJ, 301, 398
Narayanan, D., et al. 2008a, ApJ, 684, 996
Narayanan, D., et al. 2008b, ApJS, 174, 13
Riechers, D. A., et al. 2006a, ApJ, 649, 635
Riechers, D. A., et al. 2006b, ApJ, 650, 604
Riechers, D. A., Walter, F., Carilli, C. L., & Bertoldi, F. 2007, ApJ, 671, L13
Riechers, D. A., Walter, F., Brewer, B. J., Carilli, C. L., Lewis, G. F., Bertoldi, F., & Cox, P. 2008a, ApJ, 686, 851
Riechers, D. A., Walter, F., Carilli, C. L., Bertoldi, F., & Momjian, E. 2008b, ApJ, 686, L9
Riechers, D. A., Walter, F., Carilli, C. L., & Lewis, G. F. 2009, ApJ, 690, 463
Scoville, N. Z., & Sanders, D. B. 1987, Interstellar Processes (Dordrecht: Reidel)
Scoville, N. Z., et al. 1987, ApJS, 63, 821
Solomon, P. M., & Barrett, J. W. 1991, in IAU Symp. 146, Dynamics of Galaxies and Their Molecular Cloud Distributions, ed. F. Combes & F. Casoli (Dordrecht: Kluwer), 235
Spergel, D. N., et al. 2007, ApJS, 170, 377
Tacconi, L. J., et al. 2006, ApJ, 640, 228
Tacconi, L. J., et al. 2008, ApJ, 680, 246
Thompson, T. A., Quataert, E., & Murray, N. 2005, ApJ, 630, 167
Wagg, J., Wilner, D. J., Neri, R., Downes, D., & Wiklind, T. 2006, ApJ, 651, 46
Walter, F., et al. 2003, Nature, 424, 406
Walter, F., et al. 2004, ApJ, 615, L17
Walter, F., et al. 2009a, Nature, 457, 699
Walter, F., et al. 2009b, ApJ, 691, L1
Wang, R., et al. 2008, ApJ, 687, 848
Weiß, A., Downes, D., Henkel, C., & Walter, F. 2005a, A&A, 429, L25
Weiß, A., Downes, D., Walter, F., & Henkel, C. 2005b, A&A, 440, L45
Weiß, A., Henkel, C., Downes, D., & Walter, F. 2003, A&A, 409, L41

Weiß, A., Walter, F., & Scoville, N. Z. 2005c, A&A, 438, 533
Weiß, A., et al. 2007a, A&A, 467, 955
Weiß, A., et al. 2007b, in ASP Conf. Ser. 375, From Z-Machines to ALMA: (Sub) Millimeter Spectroscopy of Galaxies, ed. A. J. Baker, J. Glenn, A. I. Harris, J. G. Mangum, & M. S. Yun (San Francisco, CA: ASP), 25
Werner, M. W., et al. 1976, ApJ, 204, 420
White, R. L., Becker, R. H., Fan, X., & Strauss, M. A. 2005, AJ, 129, 2102
Willott, C. J., McLure, R. J., & Jarvis, M. J. 2003, ApJ, 587, L15
Wilson, C. D., et al. 2008, ApJS, 178, 189